Membrane-Bound Conformation of a Signal Peptide: A Transferred Nuclear Overhauser Effect Analysis†

Zhulun Wang, Jeffrey D. Jones, Josep Rizo, and Lila M. Gierasch*

Department of Pharmacology, University of Texas Southwestern Medical Center, 5323 Harry Hines Boulevard, Dallas, Texas 75235-9041

Received August 25, 1993; Revised Manuscript Received October 15, 1993®

ABSTRACT: We have determined the conformation of an analogue of the *Escherichia coli* LamB signal peptide inserted into a model membrane using the transferred nuclear Overhauser effect (trNOE) NMR technique. In order to make NMR analysis feasible, a water-soluble LamB signal peptide analogue was designed by inserting three basic residues (KRR) into the N-terminal region of the wild-type sequence (with a Val → Trp mutation for fluorescence measurements), *viz.*, MMITLR*KRR*KLPLAVAVAAG*W*M-SAQAMA-NH_2. For the purpose of the trNOE study, the binding affinity of the peptide for phospholipid vesicles was tuned by adjusting the proportion of acidic lipid in the vesicle. Circular dichroism and fluorescence measurements showed that the KRR-LamB signal peptide spontaneously inserted into the lipid bilayer with a conformational transition from a mostly random coil to a predominantly α-helical structure. The trNOE analysis revealed that the α-helix extended from approximately the beginning of the hydrophobic core (residue Leu8) to the C-terminus. The continuity of the helix was somewhat disrupted at the end of the hydrophobic core (around residue Gly17). Furthermore, the topological arrangement of the peptide within the lipid bilayer was explored by NMR line broadening induced by a paramagnetic nitroxide-labeled lipid. The line-broadening results demonstrated that the residues in the helical region are well integrated into the acyl chain region of the bilayer. The N-terminal part of the peptide showed many trNOEs, but without any indication of a helical conformation. The line-broadening analysis indicates that this part of the peptide primarily interacts with the membrane surface.

While the importance of signal sequences in protein export is well recognized (Benson et al., 1985; Randall et al., 1987; Gierasch, 1989; Gennity et al., 1990; Jones et al., 1990), the molecular mechanism by which they facilitate the translocation of polypeptide chains across membranes has not yet been elucidated. Despite their similar cellular functions, signal sequences share very little sequence homology (Watson, 1984), underlining the importance of their common structural features (Gierasch, 1989). Signal sequences generally are 15–30 residues in length with a positively charged N-terminal region, followed by a hydrophobic core of 7–12 residues and a less hydrophobic C-terminal region of 6–8 residues, which contains the cleavage site recognized by signal peptidase (von Heijne, 1985). Early studies suggested that both hydrophobicity (von Heijne, 1985) and secondary structure (Emr & Silhavy, 1983) are important for signal sequence *in vivo* function. Several properties of isolated signal peptides have been shown to correlate well with the export activity of the corresponding signal sequences *in vivo*, such as a high propensity to adopt an α-helical conformation in interfacial environments (Briggs & Gierasch, 1984; Batenburg et al., 1988a,b; McKnight et al., 1989; Rizo et al., 1993), the capacity to insert spontaneously into the acyl chain region of a phospholipid bilayer (Briggs et al., 1985; McKnight et al., 1991; Hoyt & Gierasch, 1991a; Killian et al., 1990a,b), and a mean residue hydrophobicity in the hydrophobic core above a certain threshold (Hoyt & Gierasch, 1991b; Chou & Kendall, 1990; Doud et al., 1993).

Current understanding of protein export suggests that the above properties may be important for signal sequence/membrane interaction and are certainly important for interactions of signal sequences with various proteins of the export apparatus (Wickner et al., 1991; Rapoport, 1991, 1992). The conformations of signal peptides, however, have only been studied in aqueous media and in membrane-*mimetic* environments such as aqueous trifluoroethanol (TFE[1]) and SDS detergent micelles (Bruch et al., 1989; Karslake et al., 1990; Rizo et al., 1993). The goal of the present study is to determine the conformation of a signal sequence bound to a model membrane. Future work will explore signal sequence conformations in protein-bound states.

Application of conventional solution NMR methods (Bax, 1989) to study peptides bound to a membrane bilayer is hindered by the long correlation times associated with such systems, resulting in broadening of the resonances beyond detection. In fact, only solid-state NMR techniques are capable of yielding high-resolution spectra of membrane samples since lipid bilayers and membranes are not true solutions, and their lyotropic liquid crystalline arrays cause them to show many properties of solids and semisolids (Griffin, 1981). To overcome this problem, we have performed transferred nuclear Overhauser effect (trNOE) measurements.

† This work was supported by grants from the Texas Advanced Research Fund, the NIH (GM34962 and GM29754), and the Robert A. Welch Foundation. J.D.J. was supported by an NIH postdoctoral fellowship (GM13341).

* Author to whom correspondence should be addressed.

® Abstract published in *Advance ACS Abstracts,* December 1, 1993.

[1] Abbreviations: CD, circular dichroism; DPH, diphenylhexatriene; DQF-COSY, double-quantum-filtered correlation spectroscopy; FID, free induction decay; HMQC, heteronuclear multiple-quantum coherence spectroscopy; HPLC, high-performance liquid chromatography; LamB, *E. coli* λ receptor protein; LUVs, large unilamellar vesicles; NBD, 7-nitrobenz-2-oxa-1,3-diazole; NMR, nuclear magnetic resonance; NOE, nuclear Overhauser effect; NOESY, two-dimensional nuclear Overhauser effect spectroscopy; POPC, 1-palmitoyl-2-oleoyl-*sn*-glycero-3-phosphocholine; POPG, 1-palmitoyl-2-oleoyl-*sn*-glycero-3-phosphoglycerol; 12- or 5-doxyl-PC, 1-palmitoyl-2-(5- or 12-doxyl)stearoyl-*sn*-glycero-3-phosphocholine; SDS, sodium dodecyl sulfate; SRP, signal recognition particle; *t*-Boc, *tert*-butyloxycarbonyl; TFE, 2,2,2-trifluoroethanol; TLC, thin-layer chromatography; TOCSY, two-dimensional total correlation spectroscopy; trNOE, transferred nuclear Overhauser effect.

0006-2960/93/0432-13991$04.00/0

This technique is based on the observation of NOEs between protons of a peptide in the free state that originate in the bound state and are transferred by means of chemical exchange (Clore & Gronenborn, 1982, 1983). The trNOE method has shown its power in revealing the conformation of relatively small molecules bound to macromolecules (Wakamatsu et al., 1986; Anglister & Naider, 1991; Landry et al., 1992). It is an ideal method for exploring the binding mode of peptides of the length of signal sequences to various proteins in the export machinery or to the lipid bilayer. Here, we use trNOE experiments, in conjunction with other approaches such as paramagnetic line broadening, circular dichroism (CD), and fluorescence, to explore the sequence-specific conformation of signal sequences in the membrane-bound state.

In the present study, an analogue of the LamB signal peptide was designed to facilitate NMR studies. First, it was necessary to enhance the low water solubility of signal sequences. We selected the LamB signal sequence (MMITLRKLPLA-VAVAAGVMSAQAMA) because of the availability of extensive previous results. Three basic residues (KRR) were introduced into the N-terminal region, and a tryptophan residue was substituted for a valine at position 18 of the LamB wild-type signal sequence; hence, MMITLR*KRR*KLPLA-VAVAAG*W*MSAQAMA-NH_2 (referred to as the KRR-LamB signal peptide). The addition of extra basic residues to the N-terminal region of the signal peptide is not likely to adversely affect the *in vivo* function of the corresponding signal sequence. Indeed, extra positive charges in the N-terminal region of the OmpF signal sequence increased translocation efficiency (Sasaki et al., 1990). Also, the addition of two charges to the LamB N-terminal region was phenotypically silent (T. J. Silhavy, personal communication). Thus, the modification here is most likely to correspond to a nonperturbing mutation. CD and fluorescence studies showed that the KRR-LamB signal peptide exhibited conformational tendencies and lipid interactions very similar to those of the WT signal peptide. NMR studies revealed that in the presence of LUVs composed of palmitoyloleoylphosphatidylglycerol (POPG)/palmitoyloleoylphosphatidylcholine (POPC) at a 1/99 mol % ratio, many negative trNOEs arise. The close approaches of neighboring NHs demonstrated that, in the bound state, the signal peptide is largely α-helical, as anticipated. The helix has been mapped onto the residues of the sequence on the basis of the trNOE pattern. Furthermore, the topological arrangement of the peptide in the membrane bilayer was examined by spin label-induced resonance line broadening.

EXPERIMENTAL PROCEDURES

Reagents. Synthetic 1-palmitoyl-2-oleoyl-*sn*-glycero-3-phosphocholine (POPC), 1-palmitoyl-2-oleoyl-*sn*-glycero-3-phosphoglycerol (POPG), and 1-palmitoyl-2-(5- or 12-doxyl)stearoyl-*sn*-glycero-3-phosphocholine (5- or 12-doxyl-PC) were purchased from Avanti Polar Lipids (Alabaster, AL). Lipid purity was routinely checked by thin-layer chromatography (TLC) in $CHCl_3$/MeOH/H_2O (volume ratio 65/35/5).

Peptide Synthesis and Purification. The peptide was synthesized by standard solid-phase methods (Atherton & Sheppard, 1989) on an ABI 430A peptide synthesizer (Applied Biosystems, Inc., Foster City, CA) using *t*-Boc chemistry. Purification was carried out by reverse-phase high-performance liquid chromatography (HPLC) on a Vydac phenyl column thermostated at 55 °C, with a gradient of water/acetonitrile containing 0.1% trifluoroacetic acid. The purity of the peptide was checked by analytical HPLC. The sequence and the amino acid content were verified by peptide sequencing on an ABI 477A automated sequencer (Applied Biosystems) and by quantitative amino acid analysis on a Beckman 6300 analyzer (Beckman, Fullerton, CA), respectively.

Preparation of Large Unilamellar Vesicles (LUVs). Liposomes were prepared by mixing lipids dissolved in chloroform at the desired composition. A dry lipid film was formed by evaporating the chloroform under a slow nitrogen purge followed by drying under vacuum for at least 5 h. The resulting lipid film was hydrated with the appropriate buffer. LUVs were prepared by the freeze–thaw extrusion procedure described by Hope et al. (1985). An average diameter of 90 nm can be expected from such LUVs, and there are approximately 70000–80000 lipids per vesicle. Lipid concentrations were determined by measuring the phosphorus content as described by Bartlett (1959). Signal peptides were added to preformed LUVs to make peptide/vesicle samples, thus mimicking the mode of insertion *in vivo* (i.e., from one side).

Binding Assay. The binding of the KRR-LamB signal peptide to LUVs was estimated by a centrifugation assay (Yoshimura et al., 1992). The peptide/LUV mixtures were centrifuged at 175000*g* for 5 h. The amount of the peptide in the supernatant was quantitated by amino acid analysis.

Fluorescence Measurements. An ISS Model Greg PC (ISS Inc., Champaign, IL) steady-state, photon-counting spectrofluorometer was used for the fluorescence measurements. A 1-cm-square quartz cuvette was thermostated at 25 °C with continuous stirring. Intrinsic tryptophan fluorescence emission spectra were collected from 310 to 390 nm with an excitation wavelength of 280 nm. A step size of 1 nm was used with an averaging time of 3–5 s/nm. All spectra were background corrected. The peptide concentration was either 5 or 10 μM.

The location of the tryptophan residue in the lipid bilayer was examined by spin label fluorescence quenching experiments, in which the LUVs contained a nitroxide-labeled lipid such as 5-doxyl-PC or 12-doxyl-PC. The insertion depth of the tryptophan residue in the lipid bilayer can be evaluated by comparing the fluorescence intensities of tryptophan in the presence of shallow and deep quenchers. The membrane penetration depth was estimated by the parallax method (Chattopadhyay & London, 1987; Abrams & London, 1992) according to the following equation:

$$Z_{1T} = \{-[\ln (F_1/F_2)]/(\pi C) - L_{21}^2\}/(2L_{21}) \qquad (1)$$

where Z_{1T} is the difference in depth between the shallow quencher and the tryptophan residue, F_1 and F_2 are the tryptophan fluorescence intensities in the presence of quenchers 1 (shallow) and 2 (deep), respectively, C is the quencher mole fraction per unit area, and L_{21} is the difference in depth between the two quenchers. The parameters established by Chattopadhyay and London (1987) were used in the calculation. If we assume that the surface area per lipid is 70 Å^2, that the distance of the position 2 chain carbonyl carbons to the bilayer center is 15 Å, and that the distance from the final acyl carbon to the bilayer center is 0.45 Å, the distances from the lipid bilayer surface to the 5-doxyl and 12-doxyl quenchers are 2.7 and 9.1 Å, respectively, for the spin-labeled lipids used here.

Circular Dichroism. All CD spectra were acquired in the far-UV range from 190 to 260 nm with a step size of 1 nm by using an Aviv Model 60DS or 62DS circular dichroism spectrophotometer (Aviv Associates, Inc., Lakewood, NJ). Either 1 or 0.1 mm path length quartz cells were used for the

measurements, depending on the peptide and lipid concentrations. The spectra were the average of three consecutive scans obtained with integration times of 2 or 3 s. All CD spectra shown were background corrected, converted to mean residue ellipticity, and smoothed by a polynomial fitting function (Aviv Associates, Inc.). The peptide concentration was 10 μM unless otherwise noted. CD spectra of peptides in LUVs are expected to show distortions from light scattering by the vesicles. We found that using lipid concentrations <1.5 mM minimized the distortions and yielded qualitatively interpretable peptide CD spectra.

NMR. NMR measurements were performed on a Varian VXR 500 spectrometer operating at a 500-MHz proton frequency. All 2D spectra were acquired in the phase-sensitive mode (States et al., 1982), with 6000-Hz spectral widths in both dimensions and a total of 2 × 256 free induction decays (FIDs) with 1024 complex points per FID. The mixing times were 75 ms for the total correlation spectroscopy (TOCSY) (Davis & Bax, 1985) spectra and 300 ms for the nuclear Overhauser effect spectroscopy (NOESY) (Jeener et al., 1979; Kumar et al., 1981) spectra, except in the trNOE experiments where a series of mixing times from 75 to 300 ms was used.

The 2D data were processed using the FTNMR software developed by Dennis Hare (Hare Research, Inc., Woodinville, WA) on a SUN4/260 workstation. In general, Gaussian or sine-bell apodization functions were used in both dimensions, and a matrix of 1024 × 1024 or 1024 × 4096 (for double-quantum-filtered COSY; Rance et al., 1983) real points was formed by zero-filling. The sequential assignment of the peptide was accomplished by means of TOCSY and NOESY. To confirm some assignments and solve ambiguities, ^{15}N-edited 2D NOESY-HMQC and TOCSY-HMQC spectra (Driscoll et al., 1990) were obtained on a peptide sample containing ^{15}N labels at residues Ala13 and Ala16. Line-broadening effects were assessed by double-quantum-filtered COSY measurements (Rance et al., 1983). In the DQF-COSY spectrum, the antiphase cross peaks tend to cancel each other as resonances broaden, which offers a sensitive means to monitor the broadening. Except for some experiments performed to complete the sequential assignment, all measurements were conducted at 25 °C. The chemical shifts are described in ppm relative to 3-(trimethylsilyl)propionic acid (TMSP).

RESULTS

Design of a Water-Soluble LamB Signal Sequence Analogue. In order to obtain NMR spectra with reasonable signal to noise ratios, the concentration of the peptide in solution needs to be approximately 1 mM, and the peptide must not self-associate. The limit of solubility of the native LamB signal peptide with no association is about 10-fold lower.[2] Modifications on the LamB signal peptide were therefore considered that would increase solubility but perturb the structure minimally. The aqueous solubility of polypeptides has been suggested to correlate directly with their overall hydrophobicity (Kyte & Doolittle, 1982). Addition of hydrophilic groups, charged residues typically, decreases the hydrophobicity of the peptide and, consequently, should increase the peptide solubility. Since a threshold hydrophobicity in the core region is critical to signal sequence function (Chou & Kendall, 1990; Hoyt & Gierasch, 1991b; Doud et al., 1993; Ryan et al., 1993), we elected not to alter this region. Furthermore, net charge also seems to be an important determinant for peptide solubility. Thus, addition of basic residues to the already basic N-terminal region was selected as the least perturbing modification to enhance solubility. Therefore, the KRR-LamB signal peptide was designed by placing three additional basic residues, KRR, between positions Arg6 and Lys7 in the N-terminal region of the sequence and by blocking the C-terminus. A Val → Trp substitution at residue 18, which has a wild-type export phenotype (D. Jackson & T. J. Silhavy, personal communication), was made for fluorescence studies.

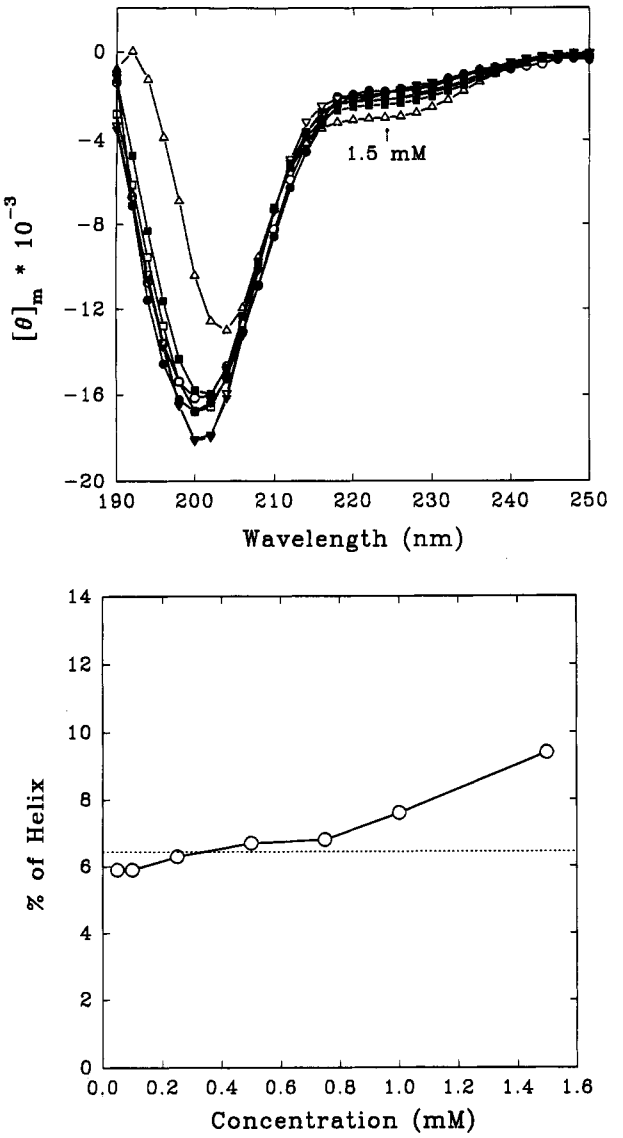

FIGURE 1: (a, top) CD spectra of the KRR-LamB signal peptide as a function of peptide concentration in 5 mM NaOAc (pH 5) buffer. The peptide concentrations were 50 μM (○), 100 μM (●), 250 μM (▽), 500 μM (▼), 750 μM (□), 1.00 mM (■) and 1.50 mM (△). (b, bottom) Corresponding concentration dependence of the estimated α-helix content of the KRR-LamB signal peptide in buffer. The percentage of α-helix was estimated from the molar ellipticity at 220 nm (Hodges et al., 1988). The dashed line indicates the average value of the α-helix content at peptide concentrations <1 mM.

Properties of the KRR-LamB Signal Peptide. CD spectra as a function of the peptide concentration were used to test the solubility of the KRR-LamB signal peptide since self-association of the peptide is usually accompanied by the formation of secondary structure. Figure 1a shows the CD spectra of the KRR-LamB signal peptide at a series of concentrations up to ~1.5 mM. The corresponding concen-

[2] Self-association of signal peptide is generally manifested as concentration-dependent changes in spectral properties, particularly CD, even when the solution is clear.

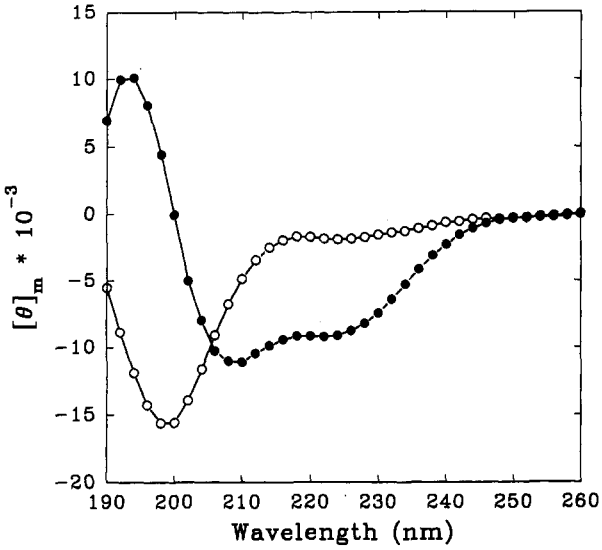

FIGURE 2: CD spectra of the KRR-LamB signal peptide in buffer (○) and in LUVs (●). The peptide concentration was 10 μM in 5 mM NaOAc (pH 5) buffer. The LUVs contained 1.5 mM lipids and 5% POPG/95% POPC (mol %).

tration dependence of the estimated α-helical content (Hodges et al., 1988) is shown in Figure 1b. Clearly, the CD spectrum of the KRR-LamB signal peptide is concentration independent up to ca. 0.8 mM, implying that the peptide is in a monomeric state. At higher concentrations, an increase in helical content is evident, which suggests association. A solubility of about 1 mM is sufficient for NMR structural studies, and thus this peptide was selected for further characterization.

Figure 2 shows the CD spectra of the KRR-LamB signal peptide in buffer (5 mM NaOAc, pH 5) and in LUVs composed of POPG/POPC at a 5/95 mol % ratio. The CD spectra show that the KRR-LamB signal peptide adopts a largely random conformation in aqueous buffer, but a substantial amount of α-helical structure is induced upon interaction with the liposomal membranes. Hence, the KRR-LamB signal peptide retains the same propensity to adopt α-helical structure in a membrane environment as the wild-type LamB signal peptide (McKnight et al., 1989). Figure 3 shows the intrinsic tryptophan fluorescence emission spectra of the KRR-LamB signal peptide in buffer and in LUVs. A typical shift in the emission maximum to lower wavelengths (blue shift) was observed upon titrating the peptide against the LUVs, which suggests that the polarity of the tryptophan environment decreased (Lakowicz, 1983). The results indicate that the KRR-LamB signal peptide retains the propensity of the WT-LamB signal peptide to insert spontaneously into the hydrophobic acyl chain region of the lipid bilayer.

Location of Trp18 in the Lipid Bilayer. The comparison of the tryptophan fluorescence emission of the KRR-LamB signal peptide in the presence of control LUVs composed of POPG/POPC (5/95 mol % ratio) with that in the presence of LUVs containing 20 mol % spin-labeled lipids (either 5-doxyl-PC or 12-doxyl-PC) is shown in Figure 4. The fluorescence is quenched by either the shallow quencher at position 5 or the deep quencher at position 12 of the lipid acyl chain, but the deep quencher quenches with higher efficiency. The ratio of quenching by the two quenchers can be used to estimate the insertion depth of the tryptophan residue. On the basis of eq 1, the penetration depth of the tryptophan residue of the KRR-LamB signal peptide in the lipid bilayer was ~8.7 Å in the LUVs of POPG/POPC at 5/95 mol % ratio with 20% spin-labeled lipid and ~8.3 Å in the LUVs

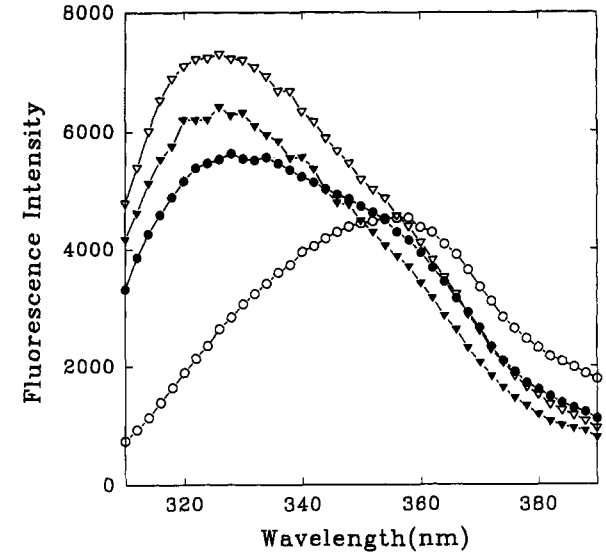

FIGURE 3: Fluorescence emission spectra of the KRR-LamB signal peptide in LUVs with different lipid concentrations. The fluorescence excitation was at a wavelength of 280 nm. The peptide concentration was 10 μM and 5% POPG/95% POPC LUVs were used. Peptide in buffer (○), peptides with lipid concentrations of 1.0 (●), 2.0 (▽), and 4.0 mM (▼). The decrease in the fluorescence intensity of the peptide in 4 mM LUVs was due to the increasing scattering by the vesicle background.

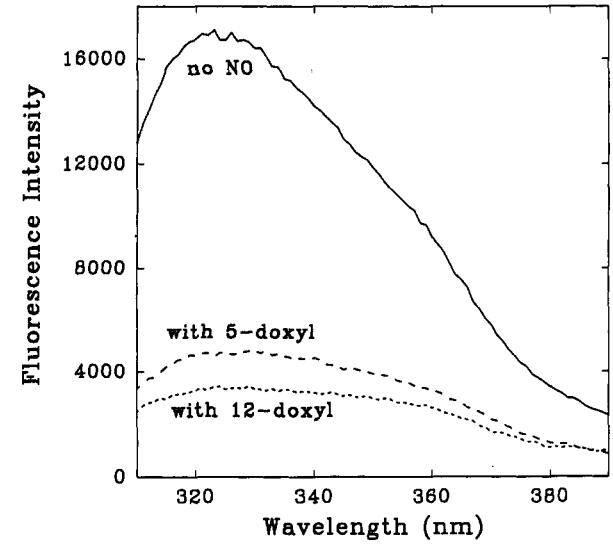

FIGURE 4: Fluorescence quenching of the KRR-LamB signal peptide in LUVs containing nitroxide spin-labeled lipid. The peptide was 10 μM in 3.0 mM LUVs. Control vesicles, 5% POPG/95% POPC (—); vesicles containing shallow quencher, 5% POPG/20% 5-doxyl-PC/75% POPC (– –); vesicles containing deep quencher, 5% POPG/20% 12-doxyl-PC/75% POPC (- - -).

of POPG/POPC at 35/65 mol % ratio with 10% spin-labeled lipid. This insertion depth is comparable to the value of ~9.0 Å observed for the tryptophan of the V18W LamB signal peptide (J. D. Jones and L. M. Gierasch, unpublished results). The accuracy of this calculation is limited because it assumes the number of spins per spin-labeled lipid to be exactly 1 and because the local spin concentration might be different from the global one. Ratios of spin to phosphate on the spin-labeled lipid from Avanti Polar Lipids have been reported in the range of 0.9 ± 0.05 (Abrams & London, 1992). Nevertheless, the position of Trp18 of the KRR-LamB signal peptide in the LUVs can be localized, at least semiquantitatively. The quenching experiment suggests that the Trp18 residue of the KRR-LamB signal peptide inserts into the acyl chain region of the bilayer and is located closer to position 12 of the acyl

chain than to position 5. The quenching result thus confirms the tryptophan fluorescence blue-shift result.

In summary, the solubility of the KRR-LamB signal peptide is enhanced enough relative to the LamB signal peptide to be sufficient for NMR studies, yet the biophysical properties of the wild-type LamB signal sequence are conserved.

Sequential Assignment of the NMR Spectrum of the KRR-LamB Signal Peptide. Sequential assignment of the proton resonances of the KRR-LamB signal peptide was hindered both by severe spectral overlap and by the lack of a preferred conformation in aqueous solution. To overcome these problems, we added a small amount (2.5 mol %) of trifluoroethanol (TFE) to the aqueous signal peptide solution to spread out the proton resonances. This quantity of TFE was still low enough to cause only small chemical shift perturbations, so that assignments could easily be correlated with the original resonance positions in the aqueous sample. The most overlapped region in the spectrum corresponded to the hydrophobic core (defined here to comprise LAVAVAA), and it was especially difficult to identify the seven alanines. Thus, the KRR-LamB signal peptide was synthesized with ^{15}N-labeled alanines at positions 13 and 16 in the sequence, enabling isotope editing to be used to resolve the overlap problem. By means of 2D ^{1}H–^{15}N TOCSY-HMQC and NOESY-HMQC, the spin systems of the two [^{15}N]Ala residues and their neighboring residues were identified. Complete sequential assignments (supplementary material) were obtained by working with the ^{15}N-labeled KRR-LamB signal peptide in 2.5 mol % (9.4% v/v) TFE/H_2O (pH 3.5) with a peptide concentration of 1.3 mM at 8 °C. The 2D NOESY and TOCSY patterns of the KRR-LamB signal peptide in aqueous buffer were then assigned by correlating corresponding cross peaks. Thus, the sequential assignments could be used for the following trNOE analysis.

Conformation of the KRR-LamB Signal Peptide in LUVs by trNOEs. Observation of trNOEs requires the ligand molecules to exchange rapidly between the bound state and the free state with respect to the spin–lattice relaxation time of the free ligand. Thus, to study the membrane-bound conformation of the signal peptide by trNOE measurements, we were obliged to tune the affinity of the peptide for the bilayer in order to achieve an off-rate in the range required for the trNOE experiments (10–10^6 s^{-1}). In addition, conditions had to be found such that vesicle stability was sufficient for the long acquisition times and relatively high peptide concentrations used in the NMR experiments. The capacity of a peptide to promote vesicle fusion has been suggested to be related primarily to two factors: association of a positively charged domain of the peptide with the surface of the bilayer, and penetration of the hydrophobic domain of the peptide into the bilayer (Defrise-Quertain et al., 1989). The KRR-LamB signal peptide has a much higher affinity for negatively charged vesicles than does the WT-LamB peptide due to the extra positive charges introduced in the N-terminal region [see Kim et al. (1991)]. The proportion of the acidic lipid, POPG, in the vesicles was thus carefully adjusted to achieve both the desired peptide affinity and vesicle stability. In addition, we found that a combination of POPG and POPC, as opposed to POPG and 1-palmitoyl-2-oleoyl-*sn*-glycero-3-phosphoethanolamine, which had been used in our previous work and better mimics the lipid composition of the *E. coli* inner membrane, decreased the tendency of the vesicles to aggregate and thus improved the stability of the peptide/vesicle samples. The conditions selected for the trNOE experiment were 0.86 mM KRR-LamB signal peptide in 15 mM LUVs composed of POPG/POPC (1/99 mol ratio) with 5 mM NaOAc (pH 5) buffer (higher salt concentration induces fusion and aggregation). The ratio of the bound peptide to the total peptide was estimated to be near 10% by the centrifugation assay.

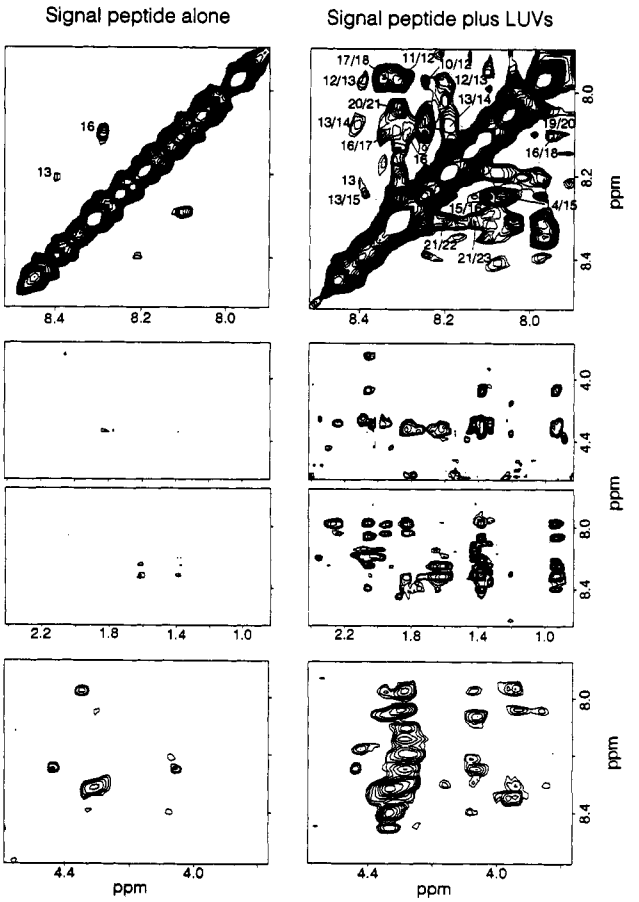

FIGURE 5: Comparison of several expanded regions of 2D NMR NOESY spectra of the KRR-LamB signal peptide in the absence (left panels) and presence of 1% POPG/99% POPC LUVs (right panels) at 25 °C. Both spectra were recorded with a 300-ms mixing time. The peptide concentration was 0.86 mM in 5 mM NaOAc (pH 5) buffer. The lipid concentration was 15 mM. All spectra displayed here were symmetrized for clarity. All expansions were plotted at the same level to facilitate comparison; additional cross peaks were seen at lower levels in the fingerprint (NH/Hα) region. Note that the amide resonances of Ala13 and Ala16 are split into two components, separated by about 0.18 ppm, due to the coupling with ^{15}N. The cross peaks observed in the amide–amide region of the peptide alone correspond to correlations between the two components of each ^{15}NH signal.

Figure 5 displays several expanded regions of the two-dimensional NOESY spectra of the KRR-LamB signal peptide in the absence and presence of the LUVs. Only a few cross peaks were observed for the KRR-LamB signal peptide in the absence of vesicles (left-hand panels in Figure 5), suggesting that the peptide lacks a specific conformation in aqueous solution and that it tumbles at a correlation time (τ_c) that gives NOEs close to zero. In the presence of the LUVs, numerous NOE cross peaks appeared for the KRR-LamB signal peptide (right-hand panels in Figure 5).[3] For the N-terminal region from Met1 to Lys7, almost no interresidue

[3] The data shown in Figure 5 correspond to NOESY experiments with a mixing time of 300 ms; trNOE experiments were obtained with mixing times of 75, 100, 150, 200, 250, and 300 ms. The build-up rates for most trNOEs are approximately linear up to a mixing time of 150–200 ms; trNOEs at a mixing time of 300 ms (shown in Figure 5) are similar in magnitude to those at 200 ms.

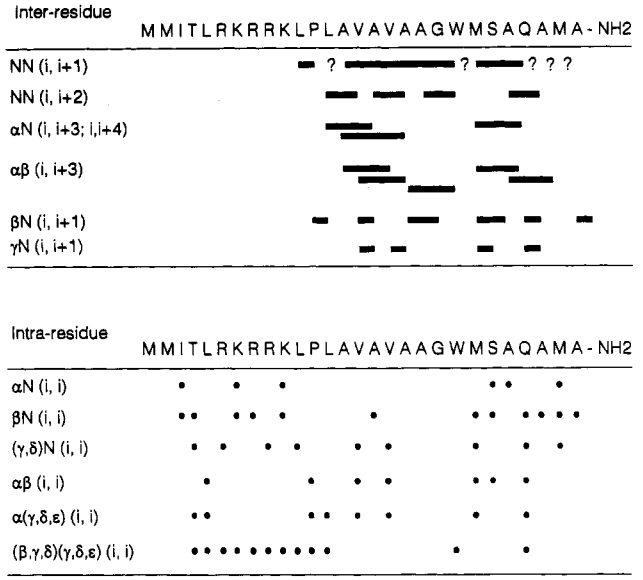

FIGURE 6: Summary of trNOEs observed for the KRR-LamB signal peptide bound to POPG/POPC LUVs (as in Figure 5). A question mark indicates amide–amide interactions that may be present, but which could not be observed due to the proximity of cross peaks to the diagonal. The interactions among aromatic protons for Trp18 are listed under $(\beta,\gamma,\delta)(\gamma,\delta,\epsilon)(i,i)$ interactions.

NOEs were observed, arguing that this part of the peptide has no preferred conformation. However, many intraresidue trNOEs were observed, suggesting that this part of the peptide was immobilized by binding to the membrane. Electrostatic interactions between the basic residues in the N-terminal part and the acidic lipid component in the membrane contribute significantly to the binding of the peptide to the membrane. The residues RKRRK are thus likely to participate in direct interactions with acidic lipids at the membrane surface, which tethers the adjacent sequence. The intraresidue trNOEs from Ile3 to Leu5 show that this part of the peptide is indeed also influenced upon binding to the slow-tumbling vesicles.

In the amide–amide region, a large number of NH(i)/NH(i+1) NOEs and several NH(i)/NH(i+2) NOEs were observed. All of these trNOEs correspond to residues in the region from residue Leu8 to the C-terminus, implying that a significant population of α-helical conformation (Wüthrich, 1986) was induced in this region. An NOE was observed between Leu8 NH and Pro9 δH, but not between Pro9 δH and Leu10 NH. The NH(i)/NH(i+1) interactions between Leu10/Ala11, Trp18/Met19, Gln22/Ala23, and Ala23/Met24 were not observable due to the similarity of their NH chemical shifts. However, NH(i)/NH(i+2) NOEs were observed between Leu10 and Val12 and between Ala21 and Ala23, and hence it is very likely that the NH(i)/NH(i+1) interactions between Leu10/Ala11 and Gln22/Ala23 exist. The α-helical conformation was confirmed by the observation of several other NOEs characteristic of α-helix, such as αH(i)/NH(i+3,4), αH(i)/βH(i+3), and βH(i)/NH(i+1) (Figure 6). No interactions characteristic of α-helix were observed between Trp18 and the residues following in the sequence. However, interactions between the aromatic 4H of Trp18 and the NH, αH, and γH of Met19 were observed (not shown). The region comprising G17W18M19 in the sequence seems to have reduced helix propensity or a kink. In summary, the observed interresidue trNOEs of the KRR-LamB signal peptide in the presence of LUVs suggest that the peptide adopts an α-helical conformation encompassing the residues from Leu8 to the C-terminus, with a slight break in the helix around Gly17 and no specific conformation for the N-terminal region.

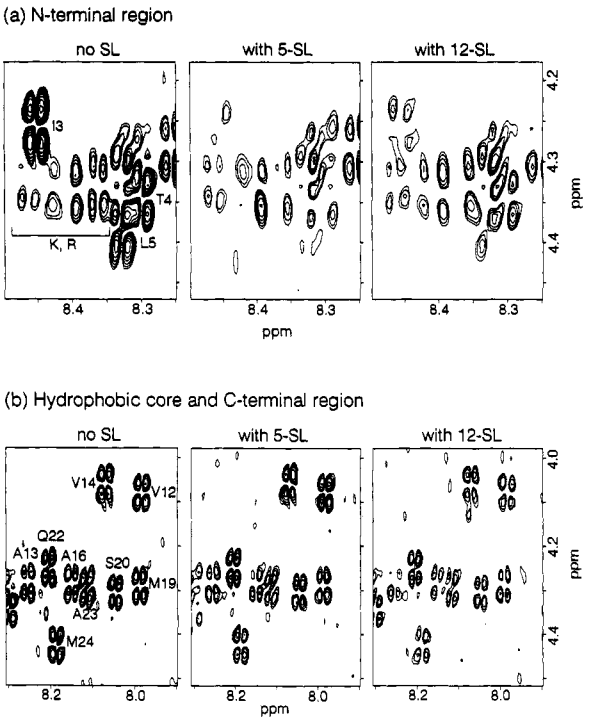

FIGURE 7: Expansion of the fingerprint regions of the 2D phase-sensitive DQF-COSY spectra of the KRR-LamB signal peptide in the presence of POPG/POPC LUVs (as in Figure 5) with or without 10% spin-labeled lipid [5-doxyl-PC (5-SL) or 12-doxyl-PC (12-SL)].

The location of the helix correlates well with previous results obtained for the WT-LamB signal peptide in TFE (Bruch et al., 1989).

Location of the KRR-LamB Signal Peptide Chain in the Lipid Bilayer. To characterize the topological arrangement of the peptide chain within the lipid bilayer, we devised a strategy analogous to spin label quenching of the Trp fluorescence described above, but taking advantage of the more detailed information available from NMR: We examined line broadening of proton resonances of the signal peptide induced by paramagnetic spin-labeled lipids incorporated into the LUVs. In like manner to the trNOE studies, broadening effects induced by the spin labels on the proton resonances of the lipid-bound peptide are transferred to the free peptide by chemical exchange. By comparing the relative broadening by shallow and deep spin-labeled lipids, the relative insertion depth of amino acid residues in the sequence can be determined.

Figure 7 shows the fingerprint (NH–αH) regions of 2D phase-sensitive DQF-COSY spectra of the KRR-LamB signal peptide in LUVs in the presence and absence of the spin-labeled lipids. Line broadening is manifested by a diminution in the intensities of the cross peaks in the presence of the spin-labeled lipids; differential loss of intensity indicates which residues are more affected by the spin labels at positions 5 or 12. Table I lists cross-peak intensities with each spin label (normalized to the intensities without spin labels) and the ratio of these intensities for the 5- and 12-position labels. Note that the N-terminal residues (up to Pro9) are more affected by either the 5- or 12-position label than are the hydrophobic core and C-terminal residues. We suggest that this differential extent of broadening reflects an alternate mode of association of the signal peptide with the bilayer that is mediated by electrostatic association of the N-terminal region with the bilayer surface and does not involve insertion of the hydrophobic core into the bilayer acyl chain region. This mode of association (which is made more likely by the excess positive charge on the KRR-LamB signal sequence) would

Table I: Approximate Penetration Depths of the KRR-LamB Signal Peptide by Spin Label-Induced Line Broadening[a]

residue	cross peak	$I_{5\text{-SL}}/I_{\text{no SL}}$	$I_{12\text{-SL}}/I_{\text{no SL}}$	$I_{5\text{-SL}}/I_{12\text{-SL}}$	depth (Å)[b]
backbone					
Ile3	NH/αH	0.19	0.34	0.56	−4.2
Thr4	NH/αH	0.32	0.52	0.62	−2.4
Arg6s	NH/αH	0.81	0.89	0.91	1.1
Pro9	δH/δH	1.00	0.88	1.14	7.5
Val12	NH/αH	0.98	0.78	1.26	9.9
Val14	NH/αH	1.04	0.78	1.33	11
Ala16	NH/αH	0.89	0.62	1.44	12
Met19	NH/αH	0.88	0.73	1.21	9.2
Ser20	NH/αH	0.90	0.76	1.18	8.9
Gln22	NH/αH	0.95	0.78	1.22	9.4
Met24	NH/αH	0.81	0.61	1.33	11
side chain					
Met1	αH/βH	0.80	0.80	1.00	5.9
Leu10	αH/βH	0.99	0.85	1.16	8.5
Trp18	4H/5H	0.70	0.59	1.19	8.9
	5H/6H	0.80	0.69	1.16	8.5
	6H/7H	0.71	0.70	1.01	6.1

[a] Conditions for acquisition of spectra and sample composition are as described in the text. The intensities used for the ratios are the average of the volume integrals of four antiphase peaks in the DQF-COSY spectrum. The reproducibility of the volume integral is ±5%, based on three independent measurements. [b] The approximate depth of penetration was calculated by eq 1 using $I_{5\text{-SL}}/I_{12\text{-SL}}$ instead of F_1/F_2; see the text for a discussion of the method and its limitations. Note that the zero plane in this formalism is at the level of the C2 of the acyl chains.

account for the increased broadening of the N-terminal residues because of their greater residence time on the bilayer. Despite the difference in residence time, the geometric relationship to the two spin labels will be revealed by the ratio between intensities when the 5- or 12-position label is present. Thus, we focus on the comparison of the broadening by 5- and 12-position spin labels in order to obtain positional information. For the residues from the hydrophobic core to the C-terminus, more broadening was seen for the 12-position spin label. Almost no broadening was observed for residues in the hydrophobic core for the 5-position spin label. This pattern of broadening suggests that most of the helical residues are well buried in the lipid acyl chain.

Since line broadening induced by proximity to a paramagnetic species has the same distance dependence as fluorescence quenching, *viz.*, r^{-6} (Mildvan & Engle, 1972), we applied the parallax method of London and co-workers (eq 1; Chattopadhyay & London, 1987; Abrams & London, 1992) to estimate the location of the broadened nuclei with respect to the bilayer. Table I also lists the results of applying the parallax method (eq 1) to the line-broadening data. Clearly, the broadening measurement reflects paramagnetic relaxation of either proton contributing to the cross peak. Hence, our estimates of depth of penetration have an intrinsic uncertainty of ca. 2.7–3.0 Å, the normal distance range betwen the NH and αH of a residue in extended or α-helical conformations. An additional approximation of this method arises because the distances were calculated using ratios between the intensities of cross peaks in DQF-COSY spectra, rather than ratios between relaxation rates produced by the spin labels.[4]

[4] We used the intensities of cross peaks in DQF-COSY spectra because they are very sensitive to line broadening. Simulations of DQF-COSY cross peak line-shapes analogous to those described in Neuhaus et al. (1985) show that, although the intensities of the cross peaks do not vary linearly with line width, the linear approximation can be assumed for a small range of line widths, such as that observed in our data. An additional approximation of our method is to consider that line width ratios are dominated by spin label-induced relaxation processes.

The side chain of the Trp18 residue provides a good test of the consistency of the results from NMR and fluorescence: The line-broadening data from the Trp aromatic ring 5H/6H COSY connectivity yields a depth of the indole of the tryptophan residue in the bilayer of about 8.5 Å from the surface, which agrees well with the fluorescence quenching results (which yielded 8.7 Å for LUVs prepared from 95/5, POPC/POPG). Moreover, using the line-broadening data clearly has the advantage that one can obtain spatial information about many sites within the peptide. The estimated locations of the residues in the hydrophobic core are 10–12 Å from the bilayer surface. For the residues in the N-terminal region, such as Ile3–Leu5, substantially more broadening was caused by the 5-position spin label than by the 12-position label. The estimated locations of Ile3 and Thr4 are about −4.2 and −2.4 Å from the surface, where the negative values indicate that they are in the headgroup or interfacial region. Thus, as discussed above, this part of the peptide probably interacts with the membrane surface in a nonspecific conformation resulting from electrostatic association of the positively charged residues with the headgroups.

DISCUSSION

Several methods of assessing the abilities of wild-type and mutant signal peptides to interact with lipid membranes have demonstrated that those peptides corresponding to functional signal sequence *in vivo* can insert spontaneously and deeply into a phospholipid membrane [for a review, see Jones et al. (1990)]. Originally, we used phospholipid monolayers to compare the insertion capabilities of LamB signal peptides (Briggs et al., 1985; McKnight et al., 1989). The maximal surface pressure increase and the concentration required to reach this level were greatest for those signal peptides with high export activities, indicating that these peptides had high affinities for the monolayer and could insert well into the acyl chain region. Similar conclusions were reached for the OmpA signal peptides using the perturbation of steady-state fluorescence polarization anisotropy of diphenylhexatriene (DPH) as an indicator of bilayer insertion (Hoyt & Gierasch, 1991a). Interestingly, the LamB signal peptides do not cause a significant increase in DPH fluorescence polarization anisotropy.

More recently, we have used Trp residues substituted at various positions within the various LamB signal peptides to analyze their membrane affinity and mode of interaction in greater detail (J. D. Jones and L. M. Gierasch, unpublished results). Both the blue shift of the Trp fluorescence and the effectiveness of quenching by spin labels introduced at different positions within the lipid acyl chains were used to assess the interaction. Comparison the affinities of mutant LamB signal peptides of differing hydrophobicity and charge revealed that much of the strength of the membrane interaction relies on electrostatic association; hydrophobicity contributes much less, but is still important. Furthermore, the parallax method of London and Chattopadhyay (1987) clearly shows that the peptides insert well within one leaflet of the bilayer (up to 10 Å depth). However, an experiment using an aqueous quencher (Tempo-choline) and fluorescently labeled wild-type LamB signal peptide [labeled with 7-nitrobenz-2-oxa-1,3-diazole (NBD) on a Cys residue at the penultimate position in the sequence] showed that the peptide does not traverse the membrane as a transmembrane helix, but instead that both termini are on the same side (the side from which it inserts); by contrast, a model transmembrane peptide (of sequence KKKKKALALALALALALALALCL-NH_2) stably

adopts the expected transmembrane arrangement by the same measurement (J. D. Jones and L. M. Gierasch, unpublished results). Experiments are in progress to test the mode of insertion of the OmpA peptides by the same approach.

Several questions clearly remain: What is the molecular conformation of the inserted signal peptide? Which residues are taking up helix when the peptide inserts? How is the helical conformation accommodated in a kinked peptide that comes back out of the bilayer on the same side? These questions demand a method that can yield an image of the conformation of the inserted signal peptide. In the present study, we have used the strategy of analyzing the NMR signals of the free peptide (present in excess) in rapid exchange with the membrane-bound peptide. The time spent in the slowly-tumbling bound state enables the efficient development of transferred NOEs (Clore & Gronenborn, 1982, 1983), which are related to interproton distances in the *bound* peptide and, thus, can yield the desired picture of the molecular conformation of the membrane-inserted peptide.

In addition to finding conditions favoring fast exchange of the signal peptide, we also had to modify the peptide to enhance its water solubility. The addition of excess positive charge at the sites of the native positively charged residues to create the KRK-LamB signal peptide adequately raised the solubility without perturbing the membrane interaction. Using membranes composed of only 1% POPG and 99% POPC as large unilamellar vesicles (LUVs) resulted in the appropriate affinity for trNOE measurements. The trNOE analysis confirmed that the peptide is largely α-helical, with the helix extending from residue 8 through the hydrophobic core and continuing to the C-terminus. The data indicate that the helix may be somewhat disrupted at the end of the hydrophobic core (near Gly17-Trp18-Met19). Similar perturbation of the helical conformation of a signal peptide was observed in the OmpA signal peptide in micelles (Rizo et al., 1993) and is consistent with the proposed role of a Pro in the signal sequence of lysozyme (Yamamoto et al., 1990; Kohara et al., 1992). The N-terminal region of the peptide is tethered to the membrane surface, as manifested by its large trNOEs, but is not part of the helix.

In addition to the information we obtained from trNOEs, we were able to use NMR to learn about the depth of insertion of the peptide in a complementary fashion to our fluorescence experiments. We incorporated spin-labeled lipids into the LUVs used in the NMR experiments and monitored line broadening of specific cross peaks in 2D spectra of the signal peptide. Increased line broadening will occur in those parts of the molecule that insert into a region close to the spin label. By comparing the effectiveness of line broadening by spin labels at different positions along the acyl chains, we could deduce the approximate depth of penetration analogously to the approach used for quenching (London & Chattopadhyay, 1987). The data from the two methods are consistent and yield a picture of the helical signal peptide inserted well into the acyl chain region, but not traversing the membrane. A looped α-helical orientation has been proposed for the signal sequence of *E. coli* outer membrane protein PhoE in the membrane-bound state (Batenburg et al., 1988a,b).

The importance of the tendency of signal peptides to insert into a bilayer must be reconciled with current knowledge of the targeting and translocation apparatus. Clearly, protein interactions are critical at the point of targeting and during translocation, and we are now actively studying the recognition of the signal sequence by SecA, SRP54, and Ffh. Nonetheless, we believe that the spontaneous insertion of the signal sequence plays a role after release of the nascent chain from SecA or SRP and before engagement of the chain with the translocation components. If so, it is important to define the conformation adopted by the signal sequence as it interacts with membrane lipids and inserts into the bilayer. The present work provides a working model from a direct NMR study of the membrane-bound signal peptide.

ACKNOWLEDGMENT

We thank Sarah Stradley for expert technical assistance in peptide synthesis and sequencing, Amy Ramin for amino acid analysis, and Muppalla Sukumar for critical reading of the manuscript.

SUPPLEMENTARY MATERIAL AVAILABLE

Table of the complete set of proton NMR assignments of the KRR-LamB signal peptide in aqueous TFE (9.4% (v/v) in pH 3.5 water, 8 °C) (2 pages). Ordering information is given on any current masthead page.

REFERENCES

Abrams, F. S., & London, E. (1992) *Biochemistry 31*, 5312–5322.
Anglister, J., & Naider, F. (1991) *Methods Enzymol. 203*, 228–241.
Atherton, E., & Sheppard, R. C. (1989) *Solid Phase Peptide Synthesis: A Practical Approach*, IRL Press, Oxford, England.
Bartlett, G. R. (1959) *J. Biol. Chem. 234*, 466–468.
Batenburg, A. M., Brasseur, R., Ruysschaert, J.-M., van Scharrenburg, G. J. M., Slotboom, A. J., Demel, R. A., & de Kruijff, B. (1988a) *J. Biol. Chem. 263*, 4202–4207.
Batenburg, A. M., Demel, R. A., Verkleij, A. J., & de Kruijff, B. (1988b) *Biochemistry 27*, 5678–5685.
Bax, A. (1989) *Annu. Rev. Biochem. 58*, 223–256.
Benson, S. A., Hall, M. N., & Silhavy, T. J. (1985) *Annu. Rev. Biochem. 54*, 101–134.
Briggs, M. S., & Gierasch, L. M. (1984) *Biochemistry 23*, 3111–3114.
Briggs, M. S., Gierasch, L. M., Zlotnick, A., Lear, J., & DeGrado, W. F. (1985) *Science 228*, 1096–1099.
Bruch, M. D., McKnight, C. J., & Gierasch, L. M. (1989) *Biochemistry 28*, 8554–8561.
Chattopadhyay, A., & London, E. (1987) *Biochemistry 26*, 39–45.
Chou, M. M., & Kendall, D. A. (1990) *J. Biol. Chem. 265*, 2873–2880.
Clore, G. M., & Gronenborn, A. M. (1982) *J. Magn. Reson. 48*, 402–417.
Clore, G. M., & Gronenborn, A. M. (1983) *J. Magn. Reson. 53*, 423–442.
Davis, D. G., & Bax, A. (1985) *J. Am. Chem. Soc. 107*, 2820–2821.
Defrise-Quertain, F., Cabiaux, V., Vandenbranden, M., Wattiez, R., Falmagne, P., & Ruysschaert, J.-M. (1989) *Biochemistry 28*, 3406–3413.
Doud, S. K., Chou, M. M., & Kendall, D. A. (1993) *Biochemistry 32*, 1251–1256.
Driscoll, P. C., Clore, G. M., Marion, D., Wingfield, P. T., & Gronenborn, A. M. (1990) *Biochemistry 29*, 3542–3556.
Emr, S. D., & Silhavy, T. J. (1983) *Proc. Natl. Acad. Sci. U.S.A. 80*, 4599–4603.
Gennity, J., Goldstein, J., & Inouye, M. (1990) *J. Bioenerg. Biomembr. 22*, 233–270.
Gierasch, L. M. (1989) *Biochemistry 28*, 923–930.
Griffin, R. G. (1981) *Methods Enzymol. 72*, 108–174.
Hodges, R. S., Semchuk, P. D., Taneja, A. K., Kay, C. M., Parker, J. M. R., & Mant, C. T. (1988) *Pept. Res. 1*, 19–30.
Hope, M. J., Bally, M. B., Webb, G., & Cullis, P. R. (1985) *Biochim. Biophys. Acta 812*, 55–65.

Hoyt, D. W., & Gierasch, L. M. (1991a) *J. Biol. Chem. 266*, 14406–14412.
Hoyt, D. W., & Gierasch, L. M. (1991b) *Biochemistry 30*, 10155–10163.
Jeener, J., Meier, B. H., Bachmann, P., & Ernst, R. R. (1979) *J. Chem. Phys. 71*, 4546–4553.
Jones, J. D., McKnight, C. J., & Gierasch, L. M. (1990) *J. Bioenerg. Biomembr. 22*, 213–232.
Karslake, C., Piotto, M. E., Pak, Y. K., Weiner, H., & Gorenstein, D. G. (1990) *Biochemistry 29*, 9872–9878.
Killian, J. A., de Jong, A. M. P., Bijvelt, J., Verkleij, A. J., & de Kruijff, B. (1990a) *EMBO J. 9*, 815–819.
Killian, J. A., Keller, R. C. A., Struyve, M., de Kroon, A. I. P. M., Tommassen, J., & de Kruijff, B. (1990b) *Biochemistry 29*, 8131–8137.
Kim, J., Mosior, M., Chung, L. A., Wu, H., & McLaughlin, S. (1991) *Biophys. J. 60*, 135–148.
Kohara, A., Yamamoto, Y., & Kikuchi, M. (1992) *FEBS Lett. 311*, 226–230.
Kumar, A., Wagner, G., Ernst, R. R., & Wüthrich, K. (1981) *J. Am. Chem. Soc. 103*, 3654–3658.
Kyte, J., & Doolittle, R. F. (1982) *J. Mol. Biol. 157*, 105–132.
Lakowicz, J. R. (1983) *Principles of Fluorescence Spectroscopy*, Plenum Press, New York.
Landry, S. J., Jordan, R., McMacken, R., & Gierasch, L. M. (1992) *Nature 355*, 455–457.
McKnight, C. J., Briggs, M. S., & Gierasch, L. M. (1989) *J. Biol. Chem. 264*, 17293–17297.
McKnight, C. J., Rafalski, M., & Gierasch, L. M. (1991) *Biochemistry 30*, 6241–6246.
Mildvan, A. S., & Engle, J. L. (1972) *Methods Enzymol. 26*, 654–682.
Neuhaus, D., Wagner, G., Vasak, M., Kagi, J. H. R., & Wüthrich, K. (1985) *Eur. J. Biochem. 151*, 257–273.
Rance, M., Sorensen, O. W., Bodenhausen, G., Wagner, G., Ernst, R. R., & Wüthrich, K. (1983) *Biochem. Biophys. Res. Commun. 117*, 479–485.
Randall, L. L., Hardy, S. J. S., & Thom, J. R. (1987) *Annu. Rev. Microbiol. 41*, 507–541.
Rapoport, T. A. (1991) *FASEB J. 5*, 2792–2798.
Rapoport, T. A. (1992) *Science 258*, 931–936.
Rizo, J., Blanco, F. J., Kobe, B., Bruch, M. D., & Gierasch, L. M. (1993) *Biochemistry 32*, 4881–4893.
Ryan, P., Robbins, A., Whealy, M., & Enquist, L. W. (1993) *Virus Genes 7*, 5–21.
Sasaki, S., Matsuyama, S., & Mizushima, S. (1990) *J. Biol. Chem. 265*, 4358–4363.
States, D. J., Haberkorn, R. A., & Ruben, D. J. (1982) *J. Magn. Reson. 48*, 286–292.
von Heijne, G. (1985) *J. Mol. Biol. 184*, 99–105.
Wakamatsu, K., Okada, A., Suzuki, M., Higashijima, T., Masui, Y., Sakakibara, S., & Miyazawa, T. (1986) *Eur. J. Biochem. 154*, 607–615.
Watson, M. E. E. (1984) *Nucleic Acids Res. 12*, 5145–5164.
Wickner, W., Driessen, A. J. M., & Hartl, F.-U. (1991) *Annu. Rev. Biochem. 60*, 101–124.
Wüthrich, K. (1986) *NMR of Proteins and Nucleic Acids*, Wiley, New York.
Yamamoto, Y., Ohkubo, T., Kohara, A., Tanaka, T., Tanaka, T., & Kikuchi, M. (1992) *Biochemistry 29*, 8998–9006.
Yoshimura, T., Goto, Y., & Aimoto, S. (1992) *Biochemistry 31*, 6119–6126.